Self-consistent electronic structure of spin-polarized dilute magnetic semiconductor quantum wells

S. P. Hong
Pusan National University, Pusan 609-735, Korea

K. S. Yi
Pusan National University, Pusan 609-735, Korea
and University of Tennessee, Knoxville, Tennessee 37996

J. J. Quinn
University of Tennessee, Knoxville, Tennessee 37996

(Received 20 May 1999; revised manuscript received 3 January 2000)

The electronic properties of spin-symmetry-broken dilute magnetic semiconductor quantum wells are investigated self-consistently at zero temperature. The spin-split subband structure and carrier concentration of modulation-doped quantum wells are examined in the presence of a strong magnetic field. The effects of exchange and correlations of electrons are included in a local-spin–density-functional approximation. We demonstrate that exchange correlation of electrons decreases the spin-split subband energy but enhances the carrier density in a spin-polarized quantum well. We also observe that as the magnetic field increases, the concentration of spin-down (majority) electrons increases but that of spin-up (minority) electrons decreases. The effect of orbital quantization on the in-plane motion of electrons is also examined and shows a sawtooth-like variation in subband electron concentrations as the magnetic-field intensity increases. The latter variation is attributed to the presence of ionized donors acting as the electron reservoir, which is partially responsible for the formation of the integer quantum Hall plateaus.

I. INTRODUCTION

Recently there has been considerable interest in magnetic semiconductor quantum structures of broken spin symmetry. The spin-polarized quantum well (SPQW) is a spin-symmetry-broken many-body system consisting of n_σ electrons of spin σ and $n_{\bar{\sigma}}$ electrons of spin $\bar{\sigma}$ embedded in a uniform positive charge background. The SPQW with arbitrary spin polarization ζ $[\zeta=(n_\sigma-n_{\bar{\sigma}})/(n_\sigma+n_{\bar{\sigma}})]$ is not a common system, unlike the spin-unpolarized electron system occurring in metal-oxide-semiconductor or modulation-doped heterostructures. The SPQW is expected to exhibit a variety of phenomena such as spin–dependent quantum confinement effects, magnetic-field-dependent carrier concentration, spin-charge-coupled excitations, and different many-body properties from that of an unpolarized electron system offering an interesting testing ground for the roles of charge and spin correlations in its many-body effects.[1–3]

A first candidate for a SPQW with tunable spin polarization ζ is a magnetic quantum well fabricated in a dilute magnetic semiconductor (DMS) structure.[4–6] A DMS structure $A_{1-x}Mn_xB$ is a mixed semiconductor crystal, in which magnetic ions (for example, Mn^{2+} or Co^{2+}) are incorporated into substitutional positions of the host ion A, in which the enhanced effective carrier g factors lead to a much larger spin splitting compared to the cyclotron frequency. In general, the ternary compound DMS has a larger band gap than that of the parent material. A quaternary compound DMS that incorporates quantum-well (QW) structures such as $ZnSe/Zn_{1-x-y}Cd_xMn_ySe/ZnSe$ (Refs. 7 and 8) is a more common SPQW system than that of a ternary compound. In a DMS SPQW structure, nonmagnetic barriers separate a dilute magnetic layer forming a two-dimensional quantum well, which is only affected by an external magnetic field.

Previously, Oparin and Quinn studied the magnetic-field dependence of the carrier concentration in a modulation-doped DMS quantum-well structure within a Hartree approximation,[2] and predicted a substantial increase in carrier concentration in the presence of a dc magnetic field. Recently, Salib *et al.* investigated the magnetoluminescence of ZnSe-based semiconductor quantum wells,[7] and demonstrated the electron-spin splitting and orbital quantization of the carriers as functions of external magnetic field.

In this paper, the electronic subband structure and carrier concentration of a spin-polarized DMS quantum well are investigated at zero temperature for various degrees of spin polarization. The effects of exchange and correlations of electrons are included within a local-spin–density-functional approximation.[9] We also examined the effect of magnetic-field-induced in-plane orbital quantization on the density of states. A strong redistribution of subband electrons is expected in the presence of orbital quantization,[10] and we observe that the effect of the orbital quantization accounts for a few-percent enhancement of the Hall plateau resistance ρ_{xy} in the integer quantum Hall effect.[11,12] In Sec. II, we present a self-consistent subband structure of the SPQW, including the effect of electron interactions. The effects of orbital quantization on the carrier concentration and spin-split subband structures are shown in Sec. III. Finally we conclude in Sec. IV.

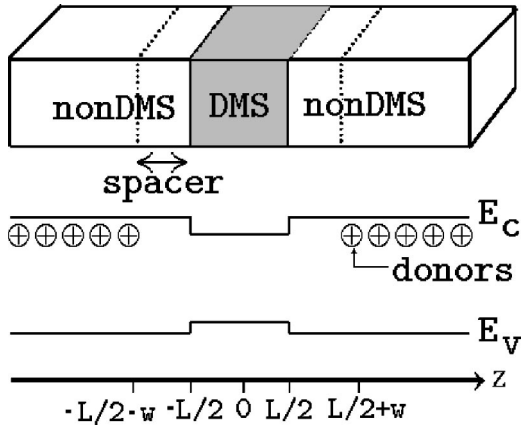

FIG. 1. Schematic diagram of a modulation-doped dilute magnetic semiconductor quantum-well structure and its band profile. The DMS layer is taken to have a smaller band gap, forming a spin-dependent quantum well.

II. SPIN-SPLIT SUBBAND STRUCTURE

We consider a modulation-doped quantum-well structure consisting of a magnetic quantum well of width L centered at the position z=0 (Fig. 1). The band gap of an alloy $A_{1-x}\mathrm{Mn}_x B$ is known, in general, to increase linearly as Mn ions are substituted into cation sites. However, we can conceive of a dilute alloy of smaller band gap compared to the host material by simply extending the linear interpolation to quaternary compounds. For an example such as $\mathrm{Zn}_{1-x-y}\mathrm{Cd}_x\mathrm{Mn}_y\mathrm{Se}$, in a simplest approximation,

$$E_g(x,y)=(1-x-y)E_g(\mathrm{ZnSe})+xE_g(\mathrm{CdSe})+yE_g(\mathrm{MnSe}). \tag{1}$$

For the case of $\mathrm{ZnSe/Zn_{0.825}Cd_{0.14}Mn_{0.035}Se/ZnSe}$, the gap energy is $E_g(0.14,0.035)=2.6845$ eV, which is smaller than that of the host material $E_g(0,0)=2.8$ eV. The nondilute magnetic layer is intentionally doped with donor impurities. Impurity-free spacer layers of a non-DMS host material of width w separate the DMS quantum well from the remainder of the host material. Although donor-free spacer layers are present, we assume that the ionized donors can serve as an electron reservoir, which makes it possible to vary the carrier concentration in the DMS layer by varying the effective dc magnetic field.

The band structure of the DMS QW region is modified by the exchange interaction of the host band electrons (i.e., the sp electron) with the localized magnetic moments (for example, the $3d^5$ electrons of Mn^{2+} ions). Such an interaction can be included formally by adding a new exchange term H_x to the original Hamiltonian H_0. The total Hamiltonian H of an electron in the DMS layer is written as

$$H=H_0+H_x. \tag{2}$$

Here H_0 and H_x are given, respectively, as

$$H_0=\frac{p^2}{2m^*}+V_0+g^*\mu_B\vec{\sigma}\cdot\vec{B} \tag{3}$$

and

$$H_x=\sum_{\vec{R}_i} J^{sp\text{-}d}(\vec{r}-\vec{R}_i)\vec{S}_i\cdot\vec{\sigma}. \tag{4}$$

The original Hamiltonian H_0 includes the band discontinuity $V_0(z)$ and the Zeeman energy $g^*\mu_B\vec{\sigma}\cdot\vec{B}$. In Eq. (4), $\vec{S}_i$ and $\vec{\sigma}$ are the spin operators of the Mn^{2+} ion and the band electron, respectively. $J^{sp\text{-}d}$ is the electron-ion sp-d exchange coupling constant. $\vec{r}$ and $\vec{R}_i$ are the coordinates of the band electron and the Mn^{2+} ion, respectively. The summation is only over the lattice sites occupied by the Mn^{2+} ions.

We adopt two convenient approximations to simplify the exchange term. Since the electronic wave function is very extended, we can expect that the electron ''sees'' a large number of Mn^{2+} ions at any time. Hence we first replace the spin operator S_i by its thermal average $\langle S\rangle$ taken over all Mn^{2+} ions. Then we approximate $J^{sp\text{-}d}(\vec{r}-\vec{R}_i)$ by $xJ^{sp\text{-}d}(\vec{r}-\vec{R})$, where x is the fraction occupancy of cation sites by magnetic ions, and $\vec{R}$ denotes the coordinate of the cation sublattice. Therefore we replace Eq. (4) by

$$H_x=\sigma_z\langle S_z\rangle x\sum_{\vec{R}} J^{sp\text{-}d}(\vec{r}-\vec{R}). \tag{5}$$

Here the summation extends over all cation sites. Then the spin-dependent part of the energy of a conduction electron is written as

$$V_B^\sigma=\sigma_z[g^*\mu_B B-N_0\eta x\langle S_z\rangle]=g_{eff}\mu_B B\sigma_z. \tag{6}$$

In the present section we confine our consideration to the case when the *effective* magnetic field B is in a direction parallel to the interface. The term $-N_0\eta x\langle S_z\rangle\sigma_z$ arises due to the exchange interaction between the conduction electron and Mn^{2+} ions: $\eta=(1/\Omega)\langle\phi|J^{sp\text{-}d}|\phi\rangle$. N_0 is the number of cation sites per unit volume, and η is the expectation value of the exchange coupling integral over a unit cell Ω.[2,6] ϕ is the wave function of a conduction electron. For conduction electrons the sign of $J^{sp\text{-}d}$ is negative.

The Schrödinger equation for an electron of spin σ in the quantum well can be written, within the Hartree approximation, by

$$\left[-\frac{\hbar^2}{2m^*}\frac{d^2}{dz^2}+V_0(z)+V_B^\sigma-e\Phi_{s.c.}(z)-E_n^\sigma\right]\chi_n^\sigma(z)=0, \tag{7}$$

where V_B^σ is the spin-dependent potential given by Eq. (6). The self-consistent potential $\Phi_{s.c}$ is the sum of the contributions arising from the electrons in the potential well and the ionized donors in the barrier. The total electronic energy is written, as shown in the Appendix, by

$$E=\sum_{i\sigma} n_i^\sigma\left[\hat{E}_i^\sigma+\frac{1}{2}(\mu-E_i^\sigma)\right], \tag{8}$$

where

$$\hat{E}_i^\sigma=E_i^\sigma-\frac{1}{2}\langle v_h(z)\rangle. \tag{9}$$

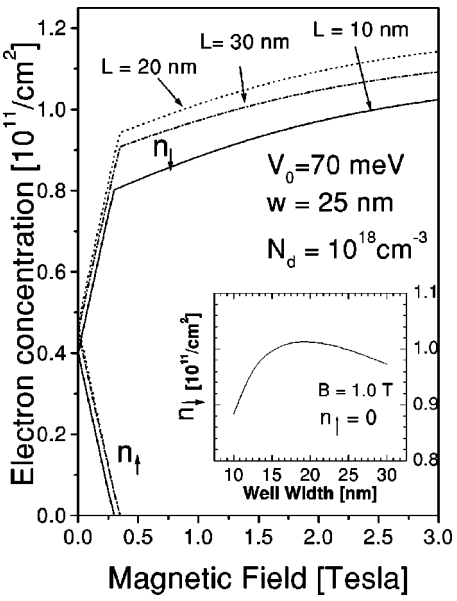

FIG. 2. Magnetic-field dependence of carrier concentrations in spin-split subbands for various widths of the semimagnetic layer, L. The effective magnetic field is taken to be along the interface of the structure. In the inset, the variation of $n_\downarrow$ is shown as a function of the width of the semimagnetic layer, L at $B=1$ T, at which the minority-spin states are empty, $n_\uparrow=0$.

The final subband energy functionals $E_1^\sigma(n_0,n_1,\ldots,n_n)$ are obtained by minimizing the total energy E. Details of the self-consistent calculation of the subband structures are given in the Appendix.

A. Carrier concentration

The electron concentration of each spin-split subband can be determined by iterating Eq. (A16) and the subband energy functional $E_i^\sigma(n_0,n_1,\ldots,n_n)$ simultaneously. We measure energies in units of $[\text{Hartree}^*]=m^*e^4/\hbar^2\epsilon^2$ and lengths in units of the effective Bohr radius $a_B^*=\hbar^2\epsilon/m^*e^2$. For the case of ZnSe ($\epsilon=8.1$, $m^*=0.17m_e$) we have 1 Hartree* $=70.5$ meV and $a_B^*=2.521$ nm. In numerical calculations, donor concentrations N_d and the sp-d exchange energy $N_0\eta x$ ($x=0.035$) were taken of the values $10^{18}/\text{cm}^3$ and 0.13 Hartree*, respectively. And the conduction-band offset is taken the case of 1 Hartree*. The thermal average $\langle S_z\rangle$, taken over all Mn^{2+} ions, is given by

$$\langle S_z\rangle=-\frac{5}{2}B_{5/2}(\xi), \tag{10}$$

where $\xi=g_{Mn}\mu_B SB/k_BT$, and $S=5/2$. Here $B_{5/2}(\xi)$ is the standard Brillouin function,[13] which approaches a value of 1 at very low temperature.

As one increases the degree of spin polarization ζ, i.e., the *effective* magnetic field B, the spin-split subband separation is expected to increase, and the total electron density in the quantum well remains constant until the spin-up (minority-spin) electron states are completely emptied. Figure 2 shows the magnetic field and the potential-well width dependence of the carrier concentrations in spin-split subbands. The electron concentrations $n_\downarrow$ and $n_\uparrow$ are obtained using the local-spin-density approximation, and displayed as a function of the *effective* magnetic field B. As the magnetic field increases, the concentration of spin-down (majority-spin) electrons increases, but that of spin-up (minority-spin) electrons decreases. The reason for this is that the well depth of spin-down electrons becomes deeper as the magnetic field increases due to the exchange interaction with Mn^{2+} ions, and finally saturates to a constant value. The variation of subband electron concentration $n_\downarrow$ is shown in the inset of Fig. 2 as a function of the width of the semimagnetic layer L of the cases $V=70$ meV and $w=25$ nm at $B=1$ T, at which the minority–spin states are all above the Fermi energy, i.e., $n_\uparrow=0$. For a quantum well of a larger conduction-band discontinuity ($V_0=98$ meV), the ground subband bottom of minority-spin electrons exceeds the chemical potential at $B_c\sim 2.5$ T.

B. Effects of carrier interactions

We examine the effect of electron-electron interaction on the subband structure employing a local-spin–density-functional approximation. We first seek electron densities of each spin, $n_\uparrow(r)$ and $n_\downarrow(r)$, for a system of n electrons interacting with one another in the SPQW beyond the Hartree approximation. These are obtained by solving Eqs. (A1) and (A2) self-consistently, including the local-spin-dependent exchange-correlation potential $v_{xc}^\sigma([n_\uparrow,n_\downarrow];z)$.

The single-particle Schrödinger equation becomes

$$\left[-\frac{\hbar^2}{2m^*}\frac{d^2}{dz^2}+V_0(z)+V_B^\sigma-e\Phi_{s.c.}+v_{xc}^\sigma(n_\uparrow,n_\downarrow;z)\right]\chi_i^\sigma(z)$$
$$=E_i^\sigma\chi_i^\sigma(z), \tag{11}$$

where σ ($=\uparrow,\downarrow$) is the z component of the spin, and i stands for the subband indices. With use of Eqs. (A5) and (A6), the total energy is now modified as follows:

$$E=\sum_{i\sigma} n_i^\sigma\left[\hat{E}_i^\sigma+\frac{1}{2}(\mu-E_i^\sigma)\right]+E_{xc}[n_\uparrow,n_\downarrow]. \tag{12}$$

In Eq. (12), the last term is the exchange-correlation energy, whose functional derivative yields the exchange-correlation potential $v_{xc}^\sigma([n_\uparrow,n_\downarrow];\vec{r})$. If the exact dependence of E_{xc} upon $n_\uparrow$ and $n_\downarrow$ were known, Eq. (12) would describe the exact ground-state energy of the spin-polarized many-electron system. In a local-spin-density (LSD) functional approximation E_{xc} is written by $E_{xc}^{LSD}[n_\uparrow,n_\downarrow]=\int d^3n(r)e_{xc}(n_\uparrow,n_\downarrow)$. Here, $e_{xc}(n_\uparrow,n_\downarrow)$ is the known exchange-correlation energy per particle for an electron gas of uniform spin densities. In the present work, we use the exchange-correlation potential suggested by Gunnarsson and Lundqvist,[9]

$$v_{xc}^\sigma=\mu_P^x(r_s)\left[\beta(r_s)\pm\frac{1}{3}\delta(r_s)\zeta/(1\pm\gamma\zeta)\right]\text{Ry}, \tag{13}$$

where $\beta(x)$ and $\delta(x)$ are defined, respectively, by $\beta(r_s)=1+0.0545r_s\ln(1+11.4/r_s)$ and $\delta(r_s)=1-0.036r_s+1.36r_s/(1+10r_s)$. Here $r_s=(3/4\pi n_e)^{1/3}$, $\gamma=0.297$, and $\mu_P^x(r_s)=-1/\pi\alpha r_s$ with $\alpha=(4/9\pi)^{1/3}$. The spin-subband energies and carrier concentrations are shown, respectively, as functions of the magnetic field in Figs. 3(a) and 3(b). The

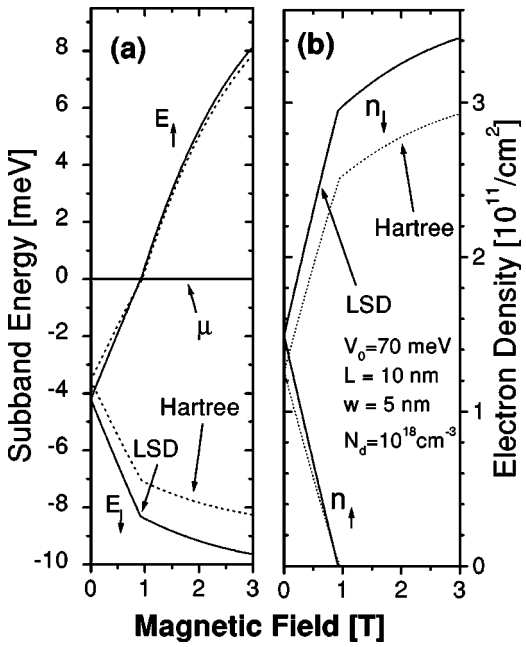

FIG. 3. The spin-split subband energies (a) and electron concentrations (b) as functions of the *effective* magnetic field taken to be parallel to the interface of the DMS layer. The solid and dotted lines are the results of the local-spin-density (LSD) functional and Hartree approximations, respectively.

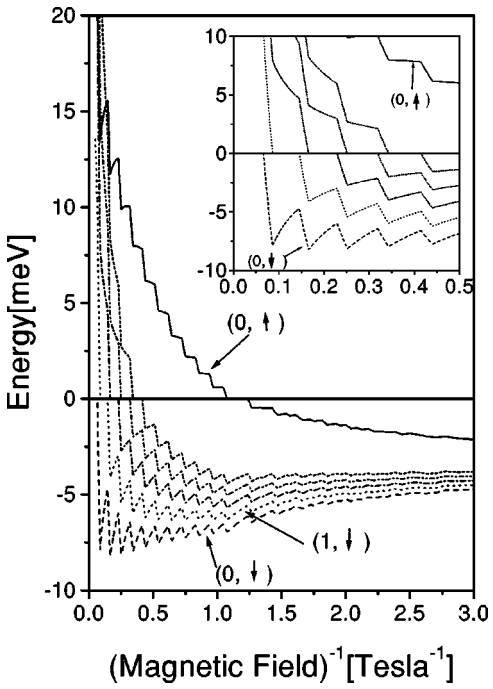

FIG. 4. The energy of each Landau level as a function of the magnetic field applied perpendicular to the quantum well. The effective magnetic field is taken to be perpendicular to the interface of the structure in order to examine the effect of orbital quantization.

energy difference $\mu - E_i^\sigma$ increases linearly with n_e, where $n_e (= n_\uparrow + n_\downarrow)$. For the case of $V_0 = 70$ meV, $L = 10$ nm, and $w = 5$ nm, the ground subband bottom of the minority-spin electrons becomes higher than the chemical potential at $B_c \sim 1$ T, and hence only spin-down states are occupied for a magnetic-field strength above 1 T. In the Hartree approximation the Coulomb repulsion of other electrons in short ranges is, in general, known to be overestimated and the effect of the exchange-correlation hole becomes more important for a small electron density $\sim 10^{11}/\mathrm{cm}^2$, lowering the Coulomb interaction energy.[14] Figure 3(a) shows that inclusion of the exchange correlations lowers the subband energy. Therefore, more electrons are expected to transfer into the quantum well due to the exchange correlations of electrons [Fig. 3(b)]. The larger spacer width gives a smaller electron density for the same reason that the larger separation of capacitors induces fewer accumulated charges. In a single-particle picture, ignoring the interaction effects altogether, i.e., neglecting both the Hartree and exchange–correlation potentials, $-e\Phi_{s.c.}$ and v_{xc}^σ in Eq. (11), the calculation does not show the complete depletion of the minority spin states at $B \geqslant 1$ T which is shown in Fig. 3. This observation implies that partial spin polarization ($\zeta < 1$) of the DMS QW would continue at higher magnetic fields in the absence of carrier interaction.

III. EFFECTS OF ORBITAL QUANTIZATION

In the presence of a strong dc magnetic field B perpendicular to the quantum well, the well-known two-dimensional density of states $\rho(\epsilon) = (m^* A/\pi\hbar^2)\Sigma_{i\sigma}\theta(\epsilon - E_i^\sigma)$ is modified in such a way that

$$\rho(\epsilon) = \sum_i \rho_i(\epsilon), \tag{14}$$

where

$$\rho_i(\epsilon) = \frac{A}{2\pi\lambda}\sum_{\nu,\sigma}\delta\left[\epsilon - E_i^\sigma - \left(\nu + \frac{1}{2}\right)\hbar\omega_c - g^*\mu_B\sigma\right]. \tag{15}$$

Here λ, ν, and A are the magnetic length $\sqrt{\hbar c/eB}$, the Landau-level index, and the area of the layer, respectively. The carrier density is given by

$$n_i = \begin{cases} Dl & \text{if } \left(l - \frac{1}{2}\right)\hbar\omega_c < \mu - E_i < \left(l + \frac{1}{2}\right)\hbar\omega_c \quad \text{(a)} \\ D(l+\tau) & \text{if } \left(l + \frac{1}{2}\right)\hbar\omega_c = \mu - E_i \quad \text{(b)}, \end{cases} \tag{16}$$

where D is the orbital degeneracy of each Landau level ($D = eB/hc$), and l and τ are the integral and fractional part of the Landau-level filling factor f, respectively ($f = l + \tau$). The case of Eq. (16b) occurs when the Fermi level lies exactly on the highest occupied Landau level.

Figure 4 shows the magnetic-field dependence of the Landau-level energies. When a Landau level is located on the chemical potential, as shown in the inset, the filling factor is fractional. For electron concentrations of $\sim 10^{11}/\mathrm{cm}^2$ and a magnetic field of 10 T, both the cyclotron energy $\hbar\omega_c$ and the Fermi energy are approximately equal to 0.1 Hartree*, and the filling factor is an order of unity. In numerical calculations we pick 1.0 Hartree* and 10 nm for V_0 and L, respectively. As one changes the magnitude of the

magnetic field B, a sawtoothlike variation is expected in the carrier concentration due to the displacement of a Landau level relative to the Fermi energy E_F. The displacement occurs for two reasons. First, its magnetic energy $(l+1/2)\hbar\omega_c$ relative to the confining potential of the quantum well increases as B increases. Second, the potential in the quantum well relative to E_F also changes with B because the electrons needed to fill the levels transfer into or out of the reservoir (ionized donors). When a Landau level is located on E_F, an increase of B raises its magnetic energy and causes the electron density to decrease; hence the Landau levels become empty, transferring electrons back to the reservoir and, thereby, lowering the potential in the quantum well. This potential lowering holds the partially filled level exactly at E_F, After the evacuation is completed, the empty level rises above E_F. Then there are no partially filled Landau levels, and the electron density starts to increase. An increase in B now increases the number of electrons allowed on each Landau level, and electrons transfer into the quantum well from the reservoir. As the potential in the quantum well rises, the magnetic energy of the Landau level rises, and the topmost filled Landau level reaches E_F. This cyclic change then repeats.

In the presence of imperfections in a sample, the density of states given by Eq. (16) is broadened, and the states in each Landau level, each of which has a degeneracy of eB/hc, are divided into two classes: localized states and extended states. If the number of electrons per unit area n_e is constant, the Fermi energy E_F jumps from one Landau level to the next with an increase in the magnetic field. When E_F lies inside the regions of localized states, the diagonal magnetoconductivity σ_{xx} becomes zero and the off-diagonal Hall conductivity becomes $\sigma_{xy}=(n_e e^2/m_e\omega_c)=f(e^2/h)$, where f is the filling factor of the Landau level. This gives rise to a region of vanishing magnetoresistance $\rho_{xx}=\sigma_{xx}/(\sigma_{xx}^2+\sigma_{xy}^2)$, and the corresponding plateau in the Hall resistance $\rho_{xy}=\sigma_{xy}/(\sigma_{xy}^2+\sigma_{xx}^2)$, at values $(h/e^2)(1/f)$, $f=1,2,3,\ldots$. This is exactly the integer quantum Hall effect.[11,12] Here a constant electron number means that only the localized states act as electron reservoirs. However, in the present work, donors in the host material are considered to act as electron reservoirs supplying electrons to the two-dimensional DMS QW. Then, as the magnetic field increases, the electron number in the well varies to establish equilibrium with the host material. With an increase in magnetic field, the Landau-level degeneracy D also increases, and hence additional quantum states are available. Those additional states are normally filled by electrons coming from the localized states, but in the present case the electrons are supplied by the ionized donors, and these electrons fill the new states. Therefore, one can observe plateaus of ρ_{xy} without localized states. In Fig. 5, we plot the inverse of the off-diagonal Hall conductivity σ_{xy}^{-1} as a function of the magnetic field. If the diagonal conductivity σ_{xx} is zero, as when the filling factor is an integer, σ_{xy}^{-1} becomes the Hall resistance ρ_{xy}. We can clearly observe plateaus at 13 and 25 T, and electron correlations enhance the width of the plateaus.[15]

IV. CONCLUSION

Self-consistent electronic properties of spin-polarized semiconductor quantum wells are investigated, including the effects of exchange and correlations of electrons in a local-spin–density-functional approximation. The spin-split electron subband structure and carrier density of modulation-doped dilute magnetic semiconductor quantum wells are examined as functions of the magnetic field. We demonstrate that exchange correlations of electrons suppress the subband energies but enhance the carrier densities in spin-polarized quantum wells. We also observe that as the magnetic field increases, the concentration of spin-down (majority-spin) electrons increases but that of spin-up (minority-spin) electrons decreases. Therefore, one could tune the spin polarization of the system by varying the strength of an effective magnetic field.

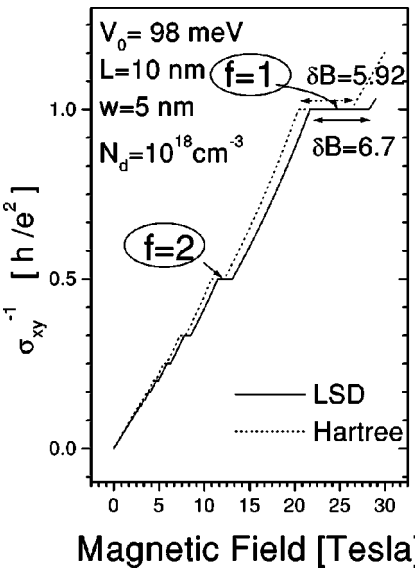

FIG. 5. Inverse off-diagonal Hall conductivity as a function of the magnetic field perpendicular to the quantum well. Dotted and solid lines, respectively, indicate the results of the Hartree and local-spin–density-functional approximations.

The orbital quantization of the in-plane motion of electrons causes sawtoothlike variation in electron density as the magnetic-field intensity increases. The latter variation is attributed to the presence of ionized donors acting as an electron reservoir, and they are demonstrated to be responsible in part for the width of the Hall plateaus. The description we are proposing is suitable for experimental observation. The broken spin symmetry of the system would introduce interesting features to its elementary excitations, such as spin-charge-coupled interspinsubband excitations. We hope that present results could be verified, for example, by far-infrared Fourier transform or resonant light scattering spectroscopy.

ACKNOWLEDGMENTS

This work was supported in part by the Korea Research Foundation through Project No. 1998-001-D00305 (S.P.H. and K.S.Y.) and by the Material Research Program of Basic Energy Sciences, U.S. Department of Energy.

APPENDIX: SELF-CONSISTENT SPIN-SPLIT SUBBAND STRUCTURES OF DMS QUANTUM WELLS

The Schrödinger equation for an electron of spin σ in the quantum well can be written, in the Hartree approximation, by

$$\left[-\frac{\hbar^2}{2m^*}\frac{d^2}{dz^2}+V_0(z)+V_B^\sigma-e\Phi_{s.c.}(z)-E_n^\sigma\right]\chi_n^\sigma(z)=0, \tag{A1}$$

where V_B^σ is the spin-dependent potential of Eq. (6). The self-consistent potential $\Phi_{s.c}$ is the sum of the contributions arising from the electrons in the potential well and the ionized donors in the barrier,

$$\frac{d^2\Phi_{s.c.}}{dz^2}=\frac{4\pi e}{\epsilon}\left[\sum_{i\sigma}^{\text{occupied}} n\sigma_i|\chi_i^\sigma(z)|^2-\sum_{R_d}\delta(r-R_d)\right], \tag{A2}$$

where n_i^σ is the areal concentration of electrons with spin σ in the ith subband, and R_d denotes the position of ionized donor impurities. We now make a typical approximation for doped semiconductors,[16]

$$\sum_{R_d}\delta(r-R_d)=\frac{1}{\Omega}\int_\Omega\delta(r-R_d)d^3R_d=N_d^+(z), \tag{A3}$$

where Ω is a macroscopic volume. Here $N_d^+(z)$ is the concentration of ionized donors. The Poisson equation to be solved together with the Schrödinger equation (A1) is written by

$$\frac{d^2\Phi_{s.c.}}{dz^2}=\frac{4\pi e}{\epsilon}\left[\sum_{i\sigma}^{\text{occupied}} n_i^\sigma|\chi_i^\sigma(z)|^2-N_d^+(z)\right]=v_h''+v_d'', \tag{A4}$$

where we have

$$v_h''=\frac{4\pi e}{\epsilon}\sum_{i\sigma} n_i^\sigma|\chi_i^\sigma(z)|^2 \tag{A5}$$

and

$$v_d''=-\frac{4\pi e}{\epsilon}N_d^+(z). \tag{A6}$$

Now, we consider the case (Fig. 1)

$$N_d^+(z)=N_d\theta\left(|z|-\frac{L}{2}-w\right)\theta\left(\frac{L}{2}+w+d-|z|\right). \tag{A7}$$

Here $\theta(x)$ denotes $\theta(x)=0$ for $x<0$; $\theta(x)=1$ for $x>0$. d is the width of the depletion layer and N_d is the average donor concentration. The chemical potential μ of the electrons, electron density n_i^σ, subband energy E_i^σ, and effective mass m_i^σ of an electron in the ith subband are related, at $T=0$ K, by

$$n_i^\sigma=\frac{m_i^\sigma}{\pi\hbar^2}(\mu-E_i^\sigma)\,\theta(\mu-E_i^\sigma). \tag{A8}$$

As a first approximation, we solve the Schrödinger equation by assuming variational wave functions of the forms

$$\chi_0^\sigma=\begin{cases}A_0^\sigma\exp\left[-\dfrac{k_0^\sigma}{2}\left(|z|-\dfrac{L}{2}\right)\right] & \text{for } |z|>\dfrac{L}{2}\\ B_0^\sigma\cos\left(\dfrac{\pi\beta_0^\sigma z}{L}\right) & \text{for } z|<\dfrac{L}{2},\end{cases} \tag{A9}$$

$$\chi_1^\sigma=\begin{cases}A_1^\sigma\exp\left[-\dfrac{k_1^\sigma}{2}\left(|z|-\dfrac{L}{2}\right)\right] & \text{for } |z|>\dfrac{L}{2}\\ B_1^\sigma\sin\left(\dfrac{\pi\beta_1^\sigma z}{L}\right) & \text{for } |z|<\dfrac{L}{2},\end{cases} \tag{A10}$$

where β_i^σ are variational parameters of the ith subband. By imposing the boundary conditions that $\chi_i^\sigma(z)$ and $(1/m^*)[d\chi_1^\sigma(z)/dz]$ are continuous at the interfaces $|z|=L/2$, and by accounting for the normalization condition, we can express A_i^σ, B_1^σ, and k_i^σ in terms of β_i^σ:

$$A_0^\sigma=B_0^\sigma\cos\left(\frac{\pi\beta_0^\sigma}{2}\right),$$

$$B_0^\sigma=\frac{\sqrt{\dfrac{2\pi\beta_0^\sigma}{L}}}{\sqrt{\pi\beta_0^\sigma+\sin(\pi\beta_0^\sigma)+2\cos^2\left(\dfrac{\pi\beta_0^\sigma}{L}\right)\cot\left(\dfrac{\pi\beta_0^\sigma}{L}\right)}}, \tag{A11}$$

$$k_0^\sigma=\frac{2\pi\beta_0^\sigma}{L}\tan\left(\frac{\pi\beta_0^\sigma}{2}\right)$$

and

TABLE I. The electron concentrations in each spin subband and the variational parameters β_n^σ for various degrees of spin polarization ζ.

ζ	$2\pi n_\downarrow$ $[a_B^{*-2}]$	$2\pi n_\uparrow$ $[a_B^{*-2}]$	$\beta_0^\downarrow$	$\beta_0^\uparrow$	$\beta_1^\downarrow$	$\beta_1^\uparrow$	$E_{10}^\downarrow$ Hartree*	$E_{10}^\uparrow$ Hartree*
0	0.0503	0.0503	0.7214	0.7214	1.3956	1.3956	0.4041	0.4041
0.2	0.0603	0.0403	0.7227	0.7202	1.3989	1.3921	0.4065	0.4015
0.4	0.0702	0.0304	0.7239	0.7189	1.4022	1.3887	0.4089	0.3989
0.6	0.0804	0.0202	0.7251	0.7176	1.4055	1.3850	0.4113	0.3962
0.8	0.0907	0.0098	0.7263	0.7163	1.4085	1.3827	0.4135	0.3937

$$A_1^\sigma = B_1^\sigma \sin\left(\frac{\pi\beta_1^\sigma}{2}\right),$$

$$B_1^\sigma = \frac{\sqrt{\frac{2\pi\beta_1^\sigma}{L}}}{\sqrt{\pi\beta_1^\sigma - \sin(\pi\beta_1^\sigma) - 2\sin^2\left(\frac{\pi\beta_1^\sigma}{L}\right)\tan\left(\frac{\pi\beta_1^\sigma}{L}\right)}}, \tag{A12}$$

$$k_1^\sigma = -\frac{2\pi\beta_1^\sigma}{L}\cot\left(\frac{\pi\beta_1^\sigma}{2}\right).$$

Since $N_d^+(z)$ has nonzero value N_d only in $L/2+w<|z|<L/2+w+d$, $v_d(z)$ is given by

$$v_d(z) = \begin{cases} 0 & \text{if } |z| < \dfrac{L}{2}+w \\ -\dfrac{2\pi e}{\epsilon} N_d \left(\dfrac{L}{2}+w-|z|\right)^2 & \text{if } \dfrac{L}{2}+w+d>|z|>\dfrac{L}{2}+w \\ \dfrac{4\pi e}{\epsilon} N_d d \left(\dfrac{L+d}{2}+w-|z|\right) & \text{if } |z| > \dfrac{L}{2}+w+d. \end{cases} \tag{A13}$$

On the other hand, $v_h(z)$, in the region $|z|<L/2$, becomes

$$v_h(z) = \sum_\sigma \left\{ \begin{array}{l} \dfrac{4\pi e n_0^\sigma}{\epsilon} B_0^{\sigma 2} \left\{ \dfrac{z^2}{4} - \dfrac{L^2}{16} + \dfrac{L^2}{8(\pi\beta_0^\sigma)^2}\left[\cos(\pi\beta_0^\sigma) - \cos\left(\dfrac{2\pi\beta_0^\sigma z}{L}\right)\right]\right\} \\ + \dfrac{4\pi e n_1^\sigma}{\epsilon} B_1^{\sigma 2} \left\{ \dfrac{z^2}{4} - \dfrac{L^2}{16} + \dfrac{L^2}{8(\pi\beta_1^\sigma)^2}\left[\cos\left(\dfrac{2\pi\beta_1^\sigma z}{L}\right) - \cos(\pi\beta_1^\sigma)\right]\right\} \end{array} \right\}, \tag{A14}$$

and, in the region $|z|>L/2$,

$$v_h(z) = \sum_\sigma \left\{ \begin{array}{l} \dfrac{4\pi e n_0^\sigma}{\epsilon} \left(\left(\dfrac{A_0^\sigma}{k_0^\sigma}\right)^2 \left\{ \exp\left[-k_0^\sigma\left(z-\dfrac{L}{2}\right)\right] - 1\right\} + \dfrac{z}{2} - \dfrac{L}{4}\right) \\ + \dfrac{4\pi e n_1^\sigma}{\epsilon} \left(\left(\dfrac{A_1^\sigma}{k_1^\sigma}\right)^2 \left\{ \exp\left[-k_1^\sigma\left(z-\dfrac{L}{2}\right)\right] - 1\right\} + \dfrac{z}{2} - \dfrac{L}{4}\right) \end{array} \right\}. \tag{A15}$$

In obtaining Eqs. (A14) and (A15) we used the physical boundary conditions $\Phi'_{s.c.}(0)=0$ and $\Phi_{s.c.}(\pm L/2)=0$, and the continuity of $v_h(z)$, $v'_h(z)$, $v_d(z)$, and $v'_d(z)$. Since the quantum well is in electrical equilibrium, we obtain the equation governing the transferred charge in equilibrium:

$$\mu = V_0 - E_d - \frac{4\pi e^2}{\epsilon} n_e \left(\frac{d}{4}+\frac{w}{2}\right) + \sum_{i\sigma} \frac{4\pi e^2 n_i^\sigma}{\epsilon}\left(\frac{A_i^\sigma}{k_i^\sigma}\right)^2. \tag{A16}$$

Here, the bulk chemical potential is taken to be pinned at the donor level. E_d and n_e are the donor binding energy and total electron density, respectively. In order to avoid double counting of the interaction energy in an evaluation of the total energy, the Hartree energy is divided by 2 to give a modified variational energy $\hat{E}_i^\sigma$. The total electronic energy is given by

$$E = \sum_{i\sigma} n_i^\sigma \left[\hat{E}_i^\sigma + \frac{1}{2}(\mu - E_i^\sigma)\right], \tag{A17}$$

where

$$\hat{E}_i^\sigma = E_i^\sigma - \frac{1}{2}\langle v_h(z)\rangle. \tag{A18}$$

The final subband energy functionals $E_1^\sigma(n_0, n_1, \ldots, n_n)$ are obtained by minimizing the total energy E. In Table I, as an example, we list numerical data obtained in the present work.[17]

[1] For example, see H. Ohno, Science **281**, 951 (1998); I. P. Smorchkova, N. Samarth, J. M. Kikkawa, and D. D. Awschalom, Phys. Rev. B **58**, 4238 (1998), and references therein.
[2] A. B. Oparin and J. J. Quinn, Solid State Commun. **98**, 791 (1996).
[3] K. S. Yi and J. J. Quinn, Phys. Rev. B **54**, 13 398 (1996); D. C. Marinescu and J. J. Quinn, *ibid.* **60**, 15 566 (1999).
[4] J. K. Furdyna, J. Appl. Phys. **64**, R29 (1988).
[5] S. Datta and J. K. Furdyna, Superlattices Microstruct. **1**, 327 (1985).
[6] J. Furdyna and J. Kossut, *Diluted Magnetic Semiconductors*, Semiconductors and Semimetals Vol. 25 (Academic Press, New York, 1988).
[7] M. S. Salib, G. Kioseoglou, H.C. Chang, H. Lou, A. Petrou, M. Dobrowolska, K. Furdyna, and A. Twardowski, Phys. Rev. B **57**, 6278 (1998).
[8] W. Heimbrodt, L. Gridneva, M. Happ, N. Hoffmann, M. Rabe, and F. Henneberger, Phys. Rev. B **58**, 1162 (1998).
[9] O. Gunarsson and B. I. Lundqvist, Phys. Rev. B **13**, 4274 (1976).
[10] G. Salis, B. Ruhstaller, K. Ensslin, K. Campman, K. Maranowski, and A. C. Gossard, Phys. Rev. B **58**, 1436 (1998), and references therein.
[11] K. V. Klitzing, Rev. Mod. Phys. **58**, 519 (1986).
[12] D. R. Yennie, Rev. Mod. Phys. **59**, 781 (1987).
[13] C. Kittel, *Introduction to Solid State Physics*, 7th ed. (Wiley, New York, 1997).
[14] Fetter and Walecka, *Quantum Theory of Many-particle Systems* (McGraw-Hill, New York, 1971).
[15] G. A. Baraff and D. C. Tsui, Phys. Rev. B **24**, 2274 (1981).
[16] G. Bastard, *Wave Mechanics Applied to Semiconductor Heterostructures* (Halsted Press, New York, 1988).
[17] W. H. Press, S. A. Teukolsky. W. T. Vetterling, and B. P. Flannery, *Numerical Recipes in C* (Cambridge University Press, Cambridge, 1993).